ELSEVIER

Journal of Nuclear Materials 266–269 (1999) 501–506

journal of nuclear materials

Determination of angle resolved velocity distributions of sputtered tungsten atoms

A. Goehlich *, N. Niemöller, H.F. Döbele

Institut f. Laser-u. Plasmaphysik, Universität Essen, Universitätstr.5, 45117Essen, Germany

Abstract

Angle resolved velocity distributions of tungsten atoms sputtered by bombardment of argon ions in the energy range between 0.2 and 5 keV are reported. The velocity distribution is determined using Doppler-shifted laser induced fluorescence spectroscopy (DSLF) in connection with a detection geometry which allows to vary the angle of emission independently of the angle of incidence. Deviations from the limiting isotropic case (Thompson distribution) are observed. Experimental velocity distributions are compared with TRIM.SP simulations.

Keywords: Sputtering; Tungsten; Laser-induced fluorescence; TRIM simulation

1. Introduction

The wall bombardment of a fusion reactor (divertor plate or limiter) with energetic particles leads – among other erosion mechanisms – to the emission of neutral particles by physical sputtering. These particles penetrate into the plasma across the magnetic field lines. The particles are ionized and the generated ions lead to a local cooling of the plasma [1] via brems- and line radiation. High-Z-materials like tungsten are considered in order to minimize this effect. The wall material tungsten has several advantages: the comparatively high threshold energy for physical sputtering is combined with a high thermal conductivity and a high ratio of the gyration radius to the ionization length, so that a local redeposition of the eroded material takes place [2]. The penetration depth into the plasma is determined by the velocity distribution of the eroded atoms which is considered here for the case of sputtering by argon ions. The velocity distribution of sputtered particles has been studied both theoretically [3,4] and experimentally [5]. The model developed by Sigmund and Thompson provides a useful reference for experiments. The basis for the applicability of this model is the developement of extended isotropic collision cascades in an amorphous solid which are typical for the bombardment of polycrystalline materials with medium mass projectiles in the keV range. The penetration depth of the ion (typically several nm) exceeds the depth of origin of the sputtered atoms (typically some Å), and the motion of the projectile is decoupled from the motion of those recoil atoms (e.g. atoms from higher collision cascade generations), which lead to the emission of atoms by collisions close to the surface. In this isotropic limiting case the velocity distribution of sputtered particles is independent of the direction and energy of the projectiles as well as of the emission angle. The resulting energy distribution of the particle flux Γ is then determined only by the height of the planar surface barrier E_b:

$$\Gamma(E) \propto \frac{E}{(E+E_b)^{n+1}}. \tag{1}$$

For hard collisions the distribution assumes the Thompson form with an energy dependence as E^{-2} for the high energy fall-off ($n=2$). This distribution is characterized by a maximum at half the surface binding energy. Deviations from the predictions of this model are observed for bombardment with light ions and/or low energies or oblique angles of incidence, since extended collision cascades can no longer develop inside

* Corresponding author. E-mail: andreas.goehlich@uni-essen.de

0022-3115/99/$ – see front matter
PII: S0022-3115(98)00830-7

the solid. Anisotropic contributions are present in addition to the isotropic fraction of the energy distribution according to Eq. (1). These contributions are linked with the momentum density deposited in the solid [6] and depend on the energy and direction of the bombarding ion. Simulation programs like the often used Monte Carlo code TRIM.SP [7] include these anisotropy corrections. The basic assumption for the applicability is also the amorphous structure of the solid, a planar surface potential and the validity of the binary collision approximation.

We report in this contribution on the measurement of velocity distributions of sputtered tungsten atoms which are emitted in definite solid angles in the polar plane. The measured distributions are compared with TRIM.SP (ver. TRVMC95).

2. Experimental

The experimental setup has been described earlier [8,9], so that a short description will be sufficient here (Fig. 1). Polycrystalline tungsten foils (ALFA, 99.95% pure), polished to high optical quality, are bombarded by argon ions. For energies between 0.2 and 1 keV a Kaufmann ion source (CSC) with current densities of approximately 100–500 $\mu A/cm^2$ is used, whereas for energies between 1 and 5 keV a Penning ion source (FISONS) is applied. The target foils are supported in a stainless steel mount with a slit, through which a laser beam can be adjusted. The free diameter of the target amounts to 8 mm (see insert in Fig. 1). The target mount is placed in the center of a vacuum vessel (base pressure 5×10^{-8} mbar) equipped with 15 suprasil Brewster windows displaced by 20° from each other. The chamber and the turbo pump are connected to the roughing pump by flexible metal bellows to allow rotation of the chamber. With this arrangement it is possible to observe the particle flux in a chosen emission direction independently of the chosen angle of incidence.

The laser beam direction and the position of the scattering volume viewed by the observation optics are spatially fixed. The emission angle of interest can be adjusted by aligning a laser window to the laser beam direction by rotation of the vacuum chamber (keeping the angle of incidence fixed). The target itself can be rotated via a vacuum stepper motor to allow changes of the angle of incidence (see insert of Fig. 1). In the following the angle of incidence (Ψ) and angle of emission in the polar plane (Φ) are measured with respect to the surface normal [see Fig. 4(a)].

The optical excitation of the tungsten atoms is performed by a pulsed laser beam generated in an excimer laser-pumped dye laser system (Lambda Physik) equipped with a second harmonic generator. The excitation wavelength is $\lambda \approx 291$ nm. The fluorescence transition at $\lambda \approx 403$ nm is observed (lifetime 93 ns). The fluorescence volume (dimension $2 \times 3 \times 3$ mm^3) is located 20 mm in front of the target surface and is imaged onto the photocathode of a Hamamatsu R928 photomultiplier; an interference filter (FWHM 5 nm) rejects false light. The fluorescence intensity is averaged in a Boxcar averager and is stored in a computer. The velocity profiles are obtained by scanning the pump radiation over the resonance line. An intracavity etalon reduces the laser linewidth corresponding to a velocity resolution of approx. 0.7 km/s. Since the resulting velocity profiles are asymmetric, a second chamber is used in which tungsten atoms are generated by sputtering in order to generate a non-Doppler-shifted fluorescence line. In this case, however, the excitation is performed perpendicular to the direction of emission. The LIF signals obtained in this reference chamber are stored together with the Doppler-shifted signals at each run. A small fraction of the pump laser intensity singled out by a beam splitter is used to normalize the signals. After cleaning for typi-

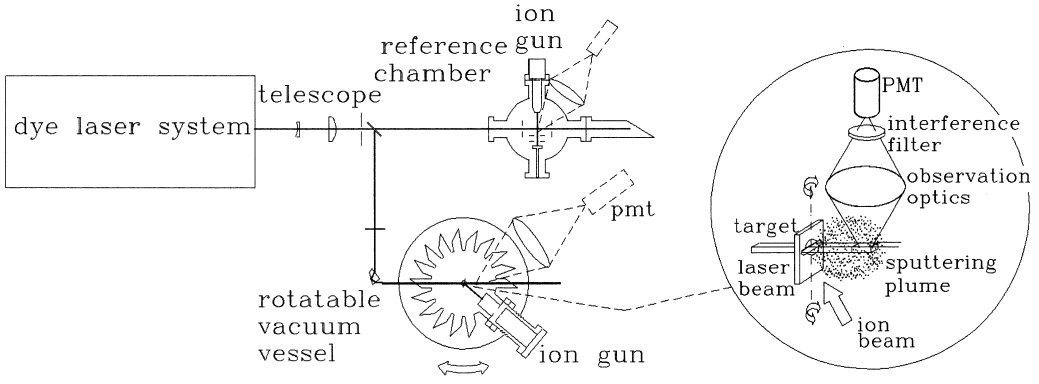

Fig. 1. Experimental setup. Details of the detection geometry are depicted in the insert. The observation optics is installed on top of the vacuum vessel.

cally 10 min by the ion beam the scanning process of the laser line is started. Depending on the signal intensity a measured point consists of 30–100 laser pulses.

3. Results and discussion

3.1. Normal incidence

Fig. 2 shows velocity distribution profiles (rectangular symbols) for different bombarding energies (argon) and normal incidence and emission.

The dashed curve represents a Thompson distribution with a surface binding energy of $E_b = 8.7$ eV (sublimation heat) for reference. The stepfunctions shown are obtained by the simulation program TRIM.SP [7]. A Krypton–Carbon interaction potential was assumed in the simulation; again a value of 8.7 eV was applied for the surface binding energy. For the inelastic energy loss with the electronic system of the solid a 50% / 50% mixture of the nonlocal Lindhard–Scharff and the local Oen–Robinson stopping power was used.

Variations of the length of the scattering volume and comparative measurements with excitation of a state with considerable shorter life time (22 ns) demonstrated that there is no influence of excited atoms leaving the scattering volume. The experimental distribution for 5 keV is well represented by a Thompson distribution with a high energy fall- off corresponding $n = 2$. The good agreement with the TRIM calculation is remarkable. The maximum of the distribution is shifted to slightly higher energies, however. If, therefore, E_b is considered as a fit parameter for a Thompson distribution (after including geometry corrections and the convolution with the laser line) a slightly higher value of $E_b = 10$ eV is obtained. At lower energies of the projectile deviations from the Thompson distribution in the high energy part of the profile are obvious. The high energy fall-off assumes a value near $n = 3$ for a bombarding energy of 300 eV. This steeper fall-off is in agreement with the simulation and is related to the higher energy loss in the few large angle collisions, which lead to sputtering in the case of low energy bombardment. Numerical solutions of the transport equations [10] exhibit the same behavior. The change of the velocity distribution with the angle of emission for normal incidence is weak (Fig. 3). This is in contrast to observations by Baxter et al.[11] who observed clear changes of the velocity distribution with the emission angle for the case of sputtering Rhodium by 5 keV argon ions at normal incidence.

3.2. Oblique incidence

The dependence on the emission angle is more pronounced for oblique incidence. Fig. 4 shows a series of measurements for an angle of incidence of $\Psi = 60°$, and

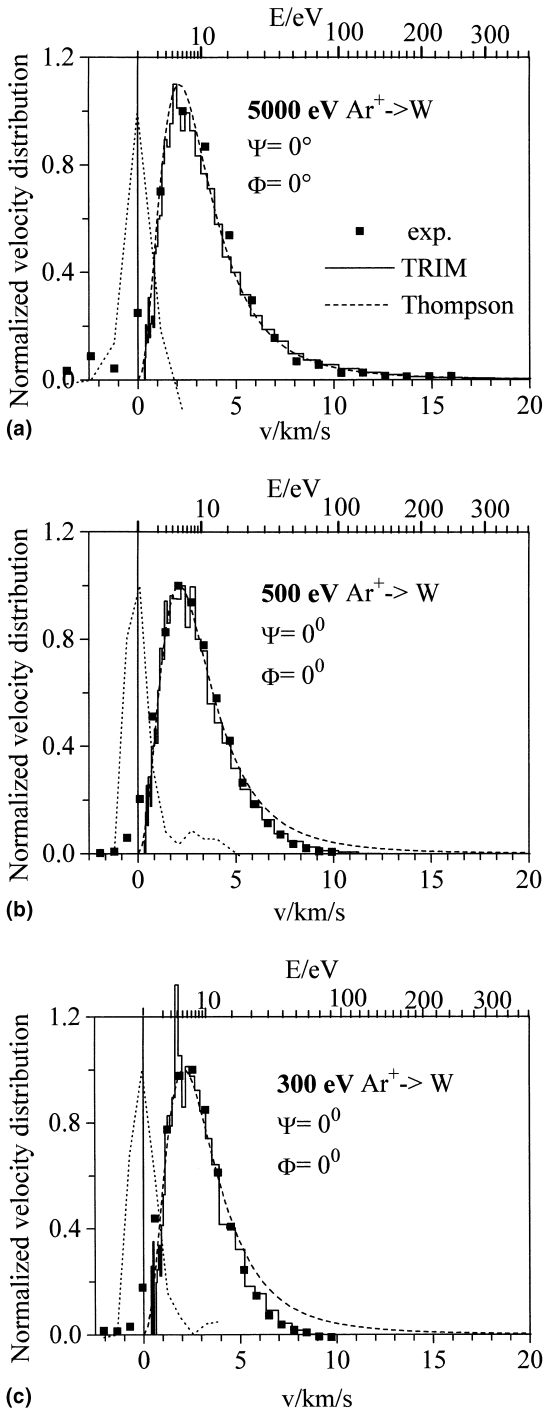

Fig. 2. Change of the velocity distributions of tungsten atoms (for normal incidence and emission) with the bombarding energy. The reference line (dotted) marking zero velocity, the TRIM simulation (solid step function) and the Sigmund–Thompson formula (dashed) are shown for comparison.

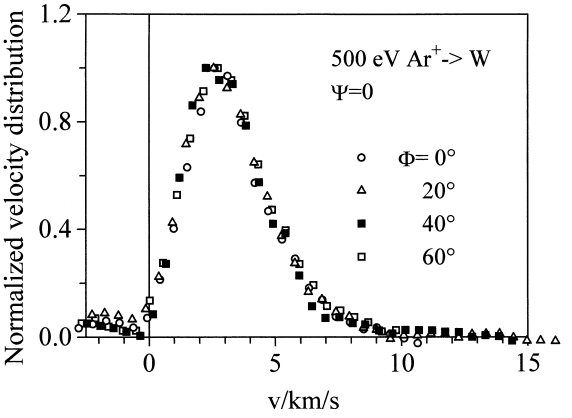

Fig. 3. Velocity distributions for normal incidence (500 eV Ar^+) and different emission angles ($\Phi = 0°$, 20°, 40°, 60°).

a bombarding energy of 500 eV. The velocity distributions in backward direction (c) and normal direction (b) are again similiar, but in forward direction (a) a shift of the maximum and a considerable broadening of the distribution is observed. The slight hump in Fig. 4(a) may be explained by the contribution of direct recoil atoms ($v_{rec} \approx 9$ km/s, indicated by an arrow). The attempt to approximate a Thompson distribution (convoluted with the laser line) would lead to a value of $E_b = 17.8$ eV for the "Thompson-parameter" E_b. Note the similiar tendency of the experimental data and the TRIM calculation. Fig. 5 demonstrates the sensitivity of our installation allowing measurements with bombarding energies as low as 200 eV. Note the change of the velocity distribution in forward direction caused by the anisotropy of the collision cascade and the stronger decrease of the distributions towards higher energy as compared to the distributions obtained for bombardment with 500 eV (Fig. 4). An approximation by the Thompson formula is no longer possible in this case.

Fig. 6(a) shows a comparison of the mean velocity obtained from the first moment of the experimental distribution with the corresponding results of the simulation for oblique bombardment with 300 eV argon ions. The corresponding data obtained for normal incidence [500 eV Ar^+ (not shown)] exhibit in the considered angular range ($0 < \Phi < 60°$) no pronounced dependence on the emission angle and give for the mean velocity a value of $v_{mean} \approx 3.3$ km/s in agreement with the TRIM.SP calculation.

The flux of the sputtered atoms as a function of the emission angle can be represented as an angular distribution [see Fig. 6(b)] on the basis of the mean velocity and the integrated absorption line profile. The corresponding TRIM.SP result is depicted by the solid line. The clear enhancement of the yield in forward direction by direct emission events is obvious. Similar observations – obtained by collector techniques – were reported

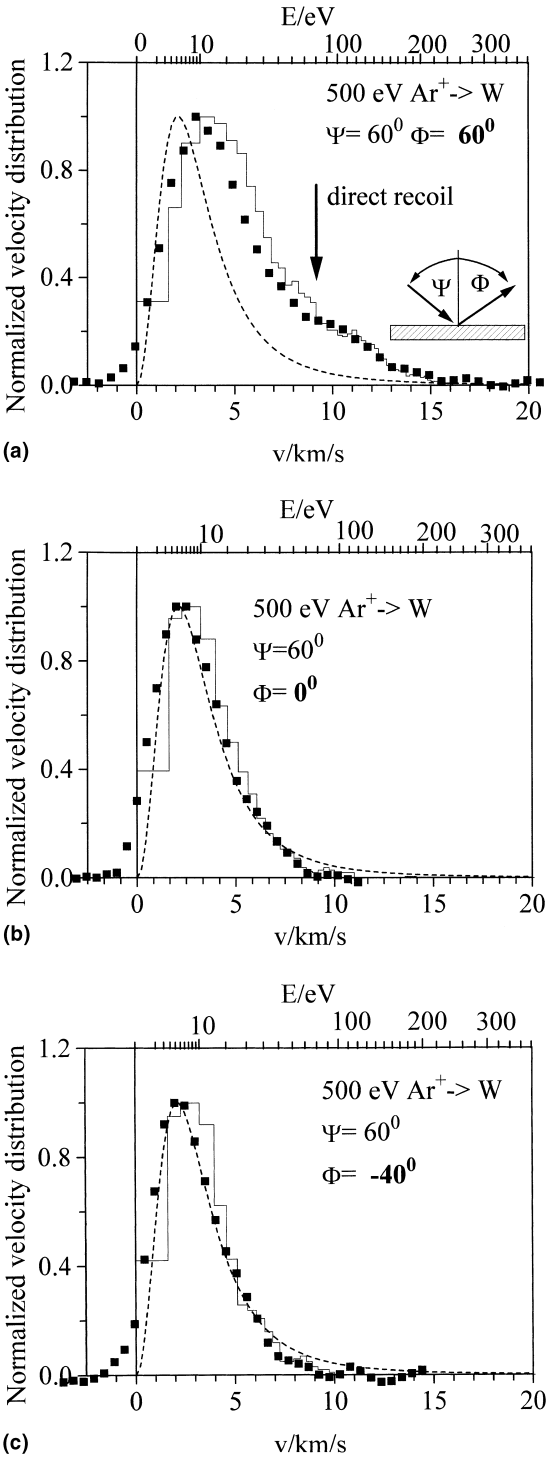

Fig. 4. Velocity distributions for oblique incidence ($\Psi = 60°$, 500 eV Ar^+). The angle of emission is varied [(a) $\Phi = 60°$, (b) $\Phi = 0°$, (c) $\Phi = -40°$].

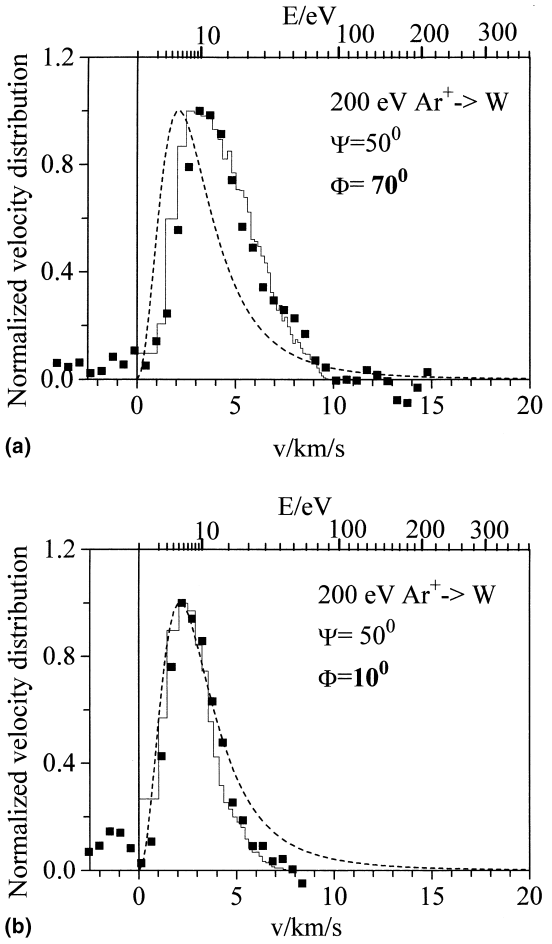

Fig. 5. Velocity distributions for oblique incidence ($\Psi = 50°$) and low bombarding energy (200 eV Ar^+) [(a) $\Phi = 70°$, (b) $\Phi = 10°$].

e.g. by Gurmin et al. [12] for the case of oblique bombardment of polycrystalline tungsten by krypton ions and by Bay et al.[13] for the case of helium bombardment in the keV range.

4. Conclusions

Experimental velocity distributions were obtained by laser induced fluorecence spectroscopy and were compared with TRIM.SP-simulations. The results for normal incidence exhibit for energies above 1 keV good agreement with the standard Sigmund–Thompson theory. Changes of the velocity distributions with the emission angle are small for normal incidence in the angular range investigated here. For oblique incidence clear changes as a function of the emission angle are obvious in agreement with the TRIM calculation. The agreement between experiment and TRIM-simulation is

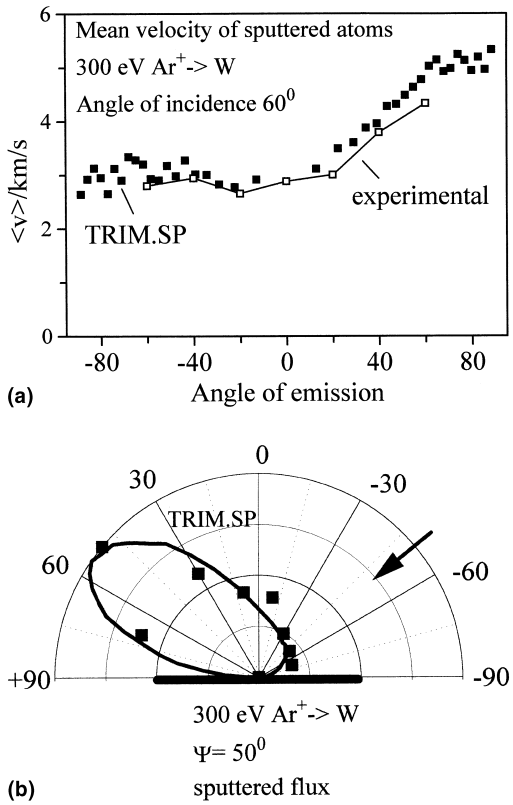

Fig. 6. Mean velocity (a) and angular flux distribution (b) compared to TRIM.SP results.

good, especially for mean velocities. This agreement with TRIM is surprising insofar as the ion bombardment induces a surface topography for the relatively high ion dose applied in this experiment (fluence up to 10^{19} cm^{-2}). SEM pictures of the bombarded surface – especially for oblique bombardment – show a roughening on a length scale of approx. 1 μm. These investigations will be continued in near future with a target mount allowing a rotation around the target normal. It is expected that with grazing incidence of the ion beam a smoothening of the surface is achieved, so that a comparison with simulations becomes more realistic e.g. with respect to the distribution of direct recoil atoms.

Acknowledgements

We thank Dr Wolfgang Eckstein from the IPP Garching for giving us the opportunity to use the TRIM.SP code.

References

[1] R. Behrisch, Atom. Plasma Mat. Interact. Data Fusion 1 (1991) 7.

[2] N. Noda, V. Phillips, R. Neu, J. Nucl. Mat. 227 (1997) 241–243.
[3] M.W. Thompson, Phys. Rep. 69 (1981) 335.
[4] P. Sigmund, Phys. Rev. 184 (1969) 383.
[5] H. Bay, Nucl. Instrum. Meth. B 18 (1987) 430.
[6] P. Sigmund, in: R. Behrisch (Ed.), Sputtering by Particle Bombardment, vol.1, Springer, Berlin, 1981.
[7] W. Eckstein, Computer Simulation of Ion–Solid Interactions, Springer, Berlin, 1991.
[8] A. Goehlich, H.F. Döbele, Nucl. Instrum. Meth. B 115 (1996) 489.
[9] A. Goehlich, N. Niemöller, J. Nucl. Mater. 241–243 (1997) 1160.
[10] M. Urbassek, Nucl. Instrum. Meth. B 4 (1984) 356.
[11] J.P. Baxter, G.A. Schick, J. Singh et al., J. Vac. Sci. Techn. A 4 (1986) 1218.
[12] B.M. Gurmin, Yu.A. Ryzhov, I.I. Shkrarban, Bull. Acad. Sci. USSR, Phys. Ser. USA 33 (1968) 752.
[13] H.L. Bay, J. Bohdansky, W.O. Hofer, J. Roth, Appl. Phys. 21 (1980) 327.